J. of Thermal Science Vol.15, No.2

Computational Analysis of a Variable Ejector Flow

H.D. KIM[1] J.H. LEE[1] T. SETOGUCHI[2] S. MATSUO[2]

1. School of Mechanical Engineering, Andong National University, 388, Songchun-dong, Andong 760-749, Korea
2. Department of Mechanical Engineering, Saga University, 1, Honjo, Saga 840-8502, Japan

The present study addresses a variable ejector which can improve the ejector efficiency and control the re-circulation ratio under a fixed operating pressure ratio. The variable ejector is a facility to obtain specific recirculation ratio under a given operating pressure ratio by varying the ejector throat area ratio. The numerical simulations are carried out to provide an understanding of the flow characteristics inside the variable ejector. The sonic and supersonic nozzles are adopted as primary driving nozzles in the ejector system, and a movable cone cylinder, inserted into a conventional ejector-diffuser system, is used to change the ejector throat area ratio. The numerical simulations are based on a fully implicit finite volume scheme of the compressible, Reynolds-Averaged Navier-Stokes equations. The results show that the variable ejector can control the recirculation ratio at a fixed operating pressure ratio.

Keywords: variable ejector, ejector throat area ratio, re-circulation ratio.

CLC number: O358 **Document code:** A **Article ID:** 1003-2169(2006)02-0140-05

Introduction

Ejector system is a facility to transport a low-pressure secondary flow by using a high-pressure primary flow. Ejector system entrains a secondary stream by a jet expansion of the primary stream in which the shear action between the primary and secondary streams arises. The performance of the ejector system is qualitatively low compared with other fluid machinery, usually driven by normal force acting on blades[1~3], however ejector system got many merits. The ejector system is simple, easy to operate and its maintenance cost is less because there are no moving parts such as valves, rotors, pistons. Ejector system has been used mainly in the field of conventional industries like the thrust augmentation of V/STOL aircraft[4,5], high-altitude state simulation facility[6], combustion facility[7], refrigeration/air conditioning[8], noise-control device[9], etc., and now it is being utilized for up-to-date technology. The representative example is the equipment for reducing the amount of hydrogen gas consumption in a hydrogen fuel-cell.

Hydrogen fuel cell generates the electric power using the reverse process of the electrolysis of water, and is one of the alternative energy sources in the near future. However, in the automobile applications of the hydrogen fuel cell system, the mileage of the vehicle is essentially limited by the amount of hydrogen fuel consumption. Thus, the automobile hydrogen fuel cell system may not be profitable, unless a means should be made to reduce the hydrogen fuel consumption.

In general, the power output of the hydrogen fuel cell system is proportional to the amount of hydrogen fuel consumption. Thus, the amount of hydrogen supply should be controlled depending upon the output power of the vehicle. In practical hydrogen fuel cell systems, some amount of hydrogen is exhausted into the air without reaction. Re-use of the exhausted hydrogen gas would be highly desirable to extend the mileage of the vehicle. In this case, it is important to control the re-circulating hydrogen gas according to the power output of the hydrogen fuel cell system.

An ejector system can be employed to re-circulate the exhausted hydrogen gas, but at a fixed pressure ratio, like the automobile hydrogen fuel cell system, the amount of re-circulating hydrogen gas is always kept constant, regardless of the output power of vehicle. Therefore, the conventional ejector system would not be suitable for the automobile hydrogen fuel cell system.

The objective of the present study is to investigate the operation characteristics of the variable sonic ejector

Received March 31, 2005

H. D.KIM: Professor

system, which can adjust the re-circulation flow by varying the ejector throat area ratio. A sonic nozzle is adopted as a primary driving nozzle, and a cone-type cylinder, which can shift upstream and downstream to alter the flow area at the ejector throat and the nozzle exit.

Experimental Methods

A convergent nozzle is selected as a primary driving nozzle for the ejector system. Fig.1 shows the configuration of the sonic nozzle. The sonic nozzle is having a circular cross section. To reduce the surface roughness effect inside the nozzle, the wall surface of the nozzle is polished. The primary driving nozzle is intruded into the ejector mixing section and designed with an angle of 24 degrees to facilitate the secondary streams.

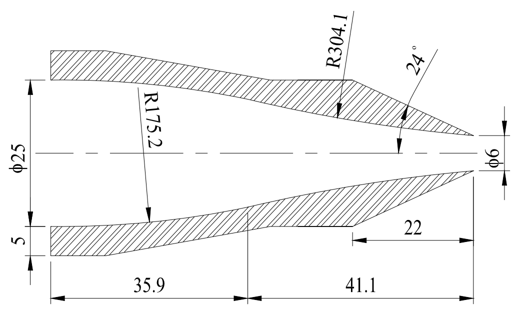

Fig.1 Sonic nozzle

For the sonic ejector the cone cylinder (cone angle = 8^0, axial length = 51.5 mm) is followed by a straight section of 400 mm length with a diameter of 8 mm. More geometric details of the cone cylinder for the variable ejector system are depicted in Fig.2.

Fig.3 shows the variable ejector in which the cone cylinder is mounted on the flow axis and supported by a strut system inside the diffuser. A screw handle installed outside the ejector is connected with the cone cylinder and is used to shift the cone cylinder. The movement of the cone cylinder changes the cross-sectional area at the nozzle throat A_{th} but the cross-sectional area at the ejector throat A_{te} is kept constant. In the present study the ejector throat area ratio ($\psi = A_{te}/A_{th}$) is greatly increased as the cone cylinder moves upstream of the exit of nozzle.

Fig.4 shows the schematic diagram of the present experimental set-up, which consists of a compressor, a reservoir, a plenum chamber, a variable ejector, and a pressure measurement system. The compressed air at 1.5 MPa in the reservoir is supplied to the primary plenum chamber, where the flow is restored to stagnation condition, and then is discharged into the ejector mixing section through the driving nozzle. The primary jet entrains the secondary flow. The resulting two streams are mixed in the mixing section and are exhausted into the atmosphere through the diffuser. The cone cylinder is facilitated to vary the ejector throat area ratio (ψ) to control the primary to secondary mass flow rate. In the present study, ψ is varied between 11.88 and 66.69. The ratio of supply pressure (p_{0p}) to the back pressure (p_a) is defined as the operating pressure ratio of the ejector, and its value is varied in the range between p_{0p}/p_a=2.0 and 9.0.

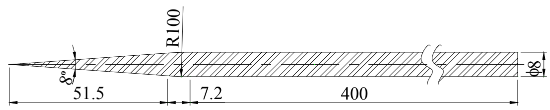

Fig.2 Cone cylinder for sonic ejector

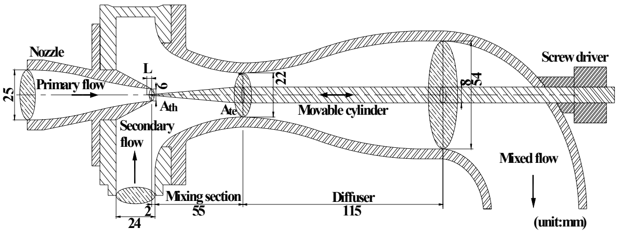

Fig.3 Schematic of the variable sonic ejector

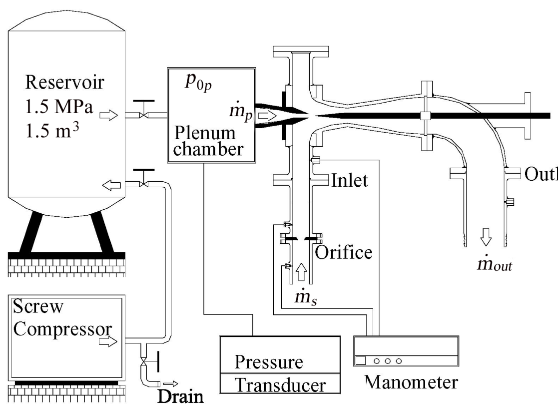

Fig.4 Schematics of the experimental set-up

The stagnation pressure is measured using a transducer, which is flush mounted on the wall of the plenum chamber. The static pressure is measured at the inlet of the secondary suction flow. In order to measure the mass flow of the secondary mass flow, an orifice system is installed at the inlet, as shown in Fig.4. The mass flow rate $\dot{m}_p$ of the primary jet is directly calculated using the pressure measured at the plenum chamber, the cross-sectional area of the primary nozzle, and the stagnation temperature. The mass flow rate $\dot{m}_s$ of the secondary suction flow is obtained from the measured pressure values p_1 and p_2, upstream and downstream of the orifice, respectively. Consequently, the coefficient C_o of discharge of the orifice is obtained from the following relationship,

$$\dot{m}_s = C_o \dot{m}_{s,\text{ideal}} = C_o \rho_2 A_2 \left\{ \frac{\frac{2\gamma}{\gamma-1}\frac{p_1}{\rho_1}\left[1-\left(\frac{p_2}{p_2}\right)^{\frac{\gamma-1}{\gamma}}\right]}{1-\left(\frac{p_2}{p_1}\right)^{\frac{2}{\lambda}}\left(\frac{A_2}{A_1}\right)^2} \right\}^{\frac{1}{2}}$$

where $\dot{m}_{s,i\text{deal}}$ is the ideal mass flow through the orifice. In order to validate the coefficient of discharge, the primary jet is discharged through the secondary flow passage while the exit of the ejector remains closed. In this situation, the mass flow rate through the orifice system is exactly the same as $\dot{m}_p$. Consequently the coefficient of discharge of the orifice is obtained as presented in Fig.5 where $\dot{m}_s$ is linearly increased with $\dot{m}_{s,\text{ideal}}$, nearly regardless of the operating pressure ratio and the ejector throat area ratio. In the present study, the coefficient of discharge C_o is obtained as 0.55.

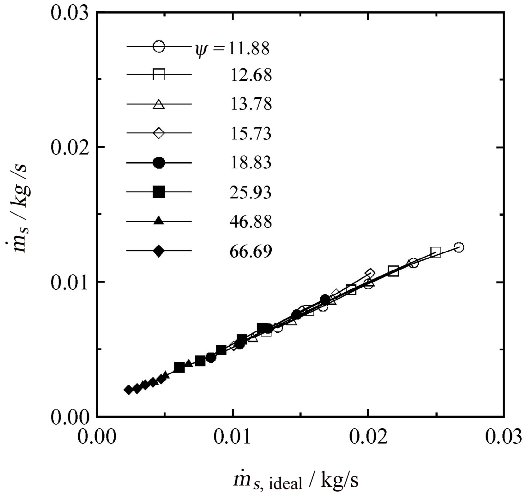

Fig.5 Relationship between $\dot{m}_s$ and $\dot{m}_{s,i\text{deal}}$

Numerical Methods

Fig.6 shows the computational grids system for the present study. The numerical simulations have been carried out with the help of a well-established standard k-omega model. The governing equations are given by the conservation forms of the 3-dimensional, symmetric, compressible Navier-Stokes equations. This model uses a control-volume based technique to convert the governing equations to algebraic equations, which can be solved numerically. The computational domain is selected based on the experimental model. As boundary conditions of computation, the pressure inlet for the upstream of the nozzle, and the pressure outlet for the secondary stream inlet and ejector outlet are applied.

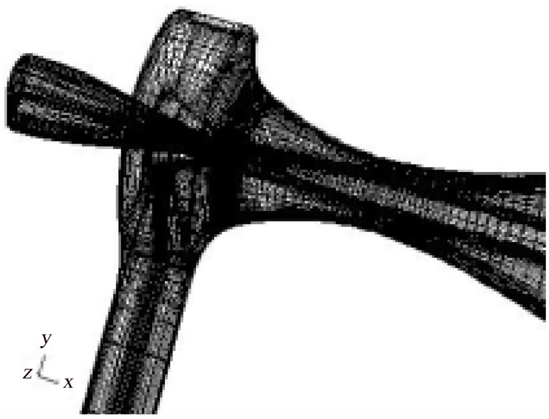

Fig.6 Computational grids system

Results and Discussion

Fig.7 shows the effects of the ejector throat area ratio and the operating pressure ratio on the re-circulation ratio of the secondary flow, where the re-circulation ratio ϕ is defined as the ratio of the secondary suction flow $\dot{m}_s$ to the total mass flow $\dot{m}_p + \dot{m}_s$ discharged from the exit of the diffuser. The dotted line shows the results of computation. It is found that at a given operating pressure ratio, ϕ increases with an increase in ψ, and ϕ appears less sensitive to p_{0p}/p_a, when ψ is small. This is because ψ affects the expansion state of the primary jet at the nozzle exit.

Fig.8 shows the velocity vectors for different throat area ratio. The operating pressure ratio of the primary nozzle was held constant by p_{0p}/p_a =2.0. The primary stream accelerates to a supersonic speed after the nozzle

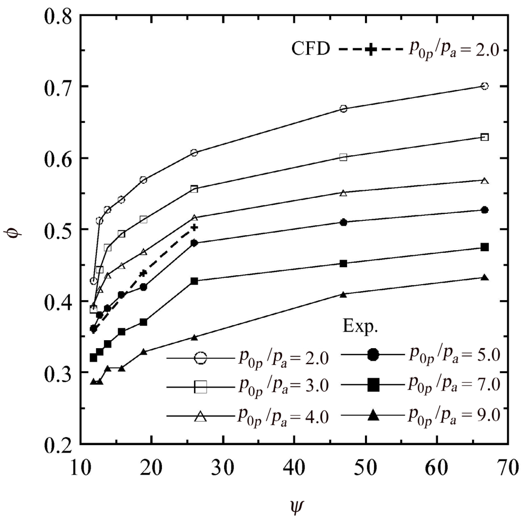

Fig.7 Relationship between ϕ and ψ

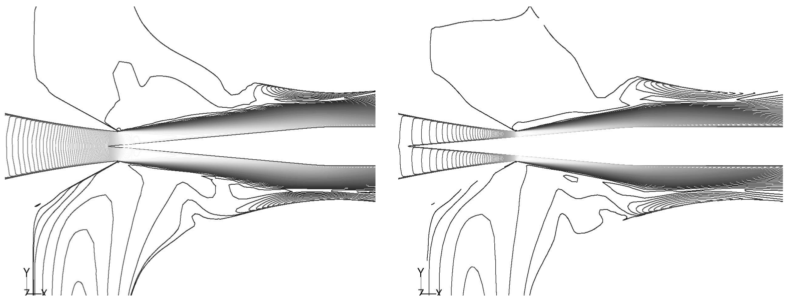

(a) ψ = 11.88   (b) ψ = 18.83   (c) ψ = 25.93

Fig.8 Velocity vectors for various ψ (p_{0p}/p_a = 2.0)

exit, resulting in an under-expanded jet zone near the cone cylinder. A barrel shock wave, which appears typical in the under-expanded jet, is a consequence of coalescence of a series of compression waves for ψ=11.88. As the ejector throat area ratio ψ increases, the barrel shock reduces to an oblique shock wave, and the zone of supersonic stream is reduced by the intrusion of the cone-cylinder resulting in the jet diffusion.

For a given ψ, the influence of p_{0p}/p_a on ϕ is shown in Fig.9. We observed that at a given ψ, ϕ decreases with an increase in p_{0p}/p_a. This tendency is somewhat different in the case of ψ=11.88, which is the smallest value in the ejector throat area ratio, applied in the present study. The present data show that for the sonic ejector, the re-circulation ratio of the secondary suction flow is strongly dependent on ψ and p_{0p}/p_a. This indicates that for a given pressure ratio of p_{0p}/p_a, the present variable sonic ejector using the present cone cylinder can control the re-circulation ratio of the secondary suction mass flow.

The variation of the secondary suction mass flow rate with the ejector throat area ratio is presented in Fig.10. The secondary suction mass flow rate monotonously decreases with ψ. However, it is interesting to note that below p_{0p}/p_a=5.0, the secondary suction mass flow rate has a maximum at a certain ψ value, which is not nearly dependent on the operating pressure ratio as p_{0p}/p_a increases. This implies that there is an optimum value of ψ for the secondary suction mass flow rate to be maximized for the sonic ejector.

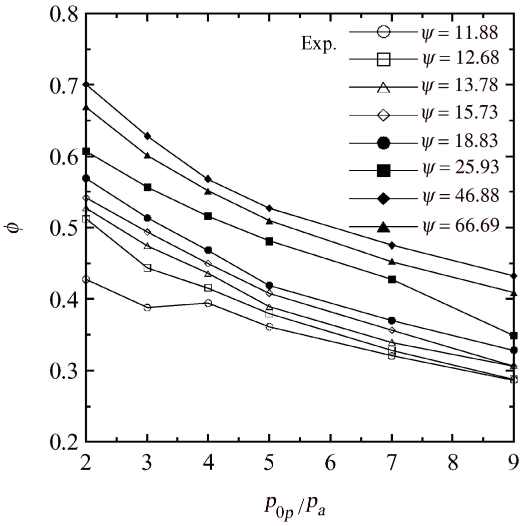

Fig.9 Relationship between ϕ and p_{0p}/p_a

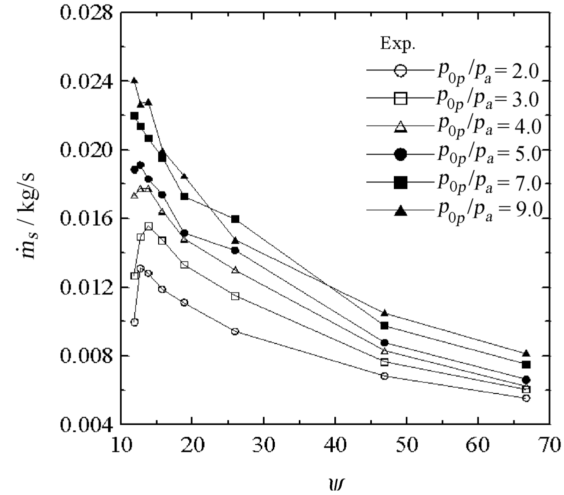

Fig.10 Secondary mass flow rate variations vs ψ

Concluding Remarks

The present study addresses the experimental and computational results of variable sonic ejector system using air as the working fluid, aiming for the application to automotive hydrogen fuel cell system. The present sonic ejector system can obtain a re-circulation ratio of the secondary suction flow required at a fixed operating pressure ratio. We concluded that for the sonic ejector, the secondary suction mass flow rate is significantly influenced by the ejector throat area ratio as well as the operating pressure ratio.

References

[1] Keenan, J H, Neumann, E P, Lustwerk, F. An Investigation of Ejector Design by Analysis and Experiment. J. of Applied Mechanics, 1950, 17(3): 299—309
[2] Presz, W M, Morin, B L, Blinn, R F. Short Efficient Ejector Systems. AIAA-87-1837, 1987
[3] Cornelius, K C, Lucius, G A. Multiple Hole Ejector Performance with Short Wide Angle Diffusers. J. of Propulsion and Power, 1994, 10(3): 369—376
[4] Alperin, M, Wu, J J. Thrust Augmenting Ejector, Part 2. AIAA Journal, 1983, 21(12): 1698—1706
[5] Yang, T T, Ntone, F, Jiang, T, et al. An Investigation of High Performances, Short Thrust Augmenting Ejectors. J. of Fluids Eng., 1985, 107: 23—30
[6] Quinn, B. Ejector Performance at High Temperatures and Pressures. J. Aircraft, 1976, 13(12): 948—954
[7] Hsu, C T. Investigation of an Ejector Heat Pump by Analytical Methods. ORNL/CON-144, Oak Ridge National Laboratory, 1984
[8] Lim, J W, Lee, S H. Engine Room Cooling System Using Jet Pump. In: Proceedings of the KSME 2000 Spring Annual Meeting B, Ulsan, 2000. 162—167
[9] Quinn, B. Interaction between Screech Tones and Ejector Performance. J. Aircraft, 1977, 14(5): 467—473

(*continued from page* 120)

[10] Sinha, M, Pinarbashi, A, Katz, J. The Flow Structure During Onset and Developed States of Rotating Stall with a Vaned Diffuser of a Centrifugal Pump. ASME J. Fluids Eng., 2001, 123: 490—499
[11] Kurokawa, J. Performance Curve Instability of a Diffuser Pump at Low Flow-Rates (in Japanese). JSME, 1988, 54(508): 3449—3456
[12] Hayami, H, Okamoto, K, Aramaki, S, et al. Development of a New Dynamic PIV System. In: Proc. of the 7th Int. Symp. of Fluid Control, Measurement and Visualization, Sorrento, 2003. 1—6
[13] Hart, D P. Super-Resolution PIV by Recursive Local-Correlation. J. of Visualization, V.S.J, 1999, 10